Supplemental material for *Laboratory Observations of Electron Heating and non-Maxwellian Distributions at the Kinetic Scale During Electron-Only Magnetic Reconnection*

Peiyun Shi,[1,*] Prabhakar Srivastav,[1] M. Hasan Barbhuiya,[1]
Paul A. Cassak,[1] Earl E. Scime,[1,†] and M. Swisdak[2]

[1]*Department of Physics and Astronomy and the Center for KINETIC Plasma Physics, West Virginia University, Morgantown, West Virginia 26506, USA*

[2]*Institute for Research in Electronics and Applied Physics, University of Maryland, College Park, Maryland 20742, USA*

(Dated: December 8, 2021)

Simulation setup and results: Here, we provide details about the simulation study of electron temperature gains for the experimental conditions. The simulations are performed using the massively parallel PIC code p3d [1] that are 2D in position-space and 3D in velocity-space. The simulation domain size is $L_X \times L_Y$ = 60 mm $\times$ 30 mm = 35.25 $d_e \times$ 17.63 d_e, which is chosen so that the distance between the X-point and O-point in the simulation in the steady-state is comparable to the experimentally determined Δ. Because the physics of electron-only reconnection is a function of system size [2], we also perform simulations with domain sizes 80 mm $\times$ 40 mm and 40 mm $\times$ 20 mm, and find the electron temperature gains are similar to the 60 mm $\times$ 30 mm case.

Unlike the experiment, the boundary conditions in the simulation are periodic and the initial conditions employ pre-existing 1D current sheets. The simulation is initiated with two current sheets, where the current is carried solely by electrons. The reconnecting magnetic field is $B_X = B_{recx}\{\tanh\left[(Y-0.25L_Y)/w_0\right] - \tanh\left[(Y-0.75L_Y)/w_0\right] - 1\}$ where $B_{recx} = 15$ G is the asymptotic reconnecting field strength and $w_0 = 1.25$ mm is the thickness of the initial current sheet. Initially, both electron and ion densities have a profile given by $n(Y) = n_{CS}\left\{\mathrm{sech}^2\left[(Y-L_Y/4)/w_0\right] + \mathrm{sech}^2\left[(Y-3L_Y)/4w_0\right]\right\} + n_{BG}$. Here, $n_{BG} = 1 \times 10^{13}$ cm^{-3} is the asymptotic upstream density, $n_{CS} = B_{recx}^2/[8\pi k_B(T_e+T_i)] = 0.2\ n_{BG}$ is the peak density of the current sheet population, and the initial electron T_e and ion T_i temperature are 2.45 eV and 0.49 eV, respectively, as motivated by the experiments. The guide field is initially uniform with $B_g = 25\ B_{recx} = 375$ G.

We use the realistic electron-to-argon ion mass ratio $m_e/m_i = 1/72{,}900$. The time step $\Delta t = 2.67 \times 10^{-2}$ ns = $7 \times 10^{-3}\ \Omega_{ce}^{-1}$. The grid-length $\Delta x = 3.9 \times 10^{-3}$ cm, which is significantly smaller than the smallest length-scale in the system, the Debye length $\lambda_D \simeq \lambda_{Di} = (\varepsilon_0 k_B T_i/n_{BG}e^2)^{1/2} = 9.9 \times 10^{-3}$ cm = 0.06 d_e based on the upstream density n_{BG}. The speed of light is chosen to be an unrealistic value of $c = 4.4 \times 10^6$ m/s = 10 $c_{Ae,recx}$, where $c_{Ae,recx} = B_{recx}/(\mu_0 m_e n_{BG})^{1/2}$, because a realistic choice for c would significantly increase the computational run time. We do not anticipate this choice modifies the physics of interest, as the system is non-relativistic. Unlike the experiment, the simulations are collisionless. This is not expected to greatly impact the results since the experiment is marginally collisional at most. There are 2048 $\times$ 1024 grid cells with 200 weighted particles per grid element. The current sheet readily reconnects when seeded with a small magnetic perturbation. We study the lower current sheet because it does not produce secondary

* peiyun.shi@mail.wvu.edu

† earl.scime@mail.wvu.edu

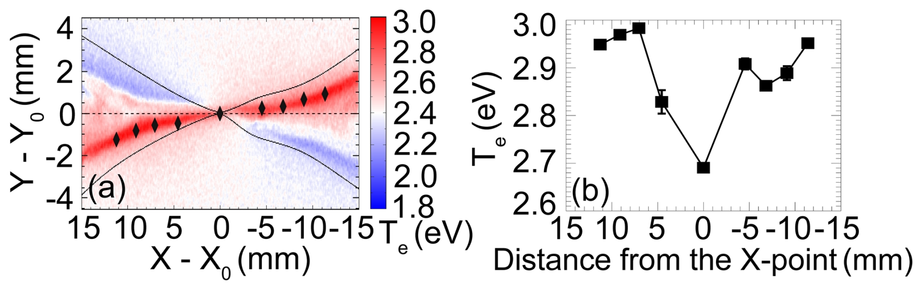

Fig. S 1. PIC simulation result of electron temperature T_e. (a) 2D-profile. (b) T_e at the locations shown by black diamonds in (a) as a function of distance from the X-point.

islands.

Fig. S1(a) shows the 2D profile of T_e at $t = 1.2\ \mu$s, where we define the location of the X-point as (X_0, Y_0) and plot data relative to that point. Electron heating is enhanced along one of the two separatrices as is typical for reconnection with a strong guide field [3, 4]. This heating happens in a narrow region of thickness $\simeq 1$ mm $\simeq 0.6\ d_e \simeq 7\ \rho_e$. Fig. S1(b) shows T_e at the locations marked in panel (a) as a function of distance from the X-point, identical to the Fig. 1(c) in the letter. It shows that T_e increases with distance from X-point and it is in excellent qualitative and reasonable quantitative agreement with the experiment (see Fig. 2(b) in the letter). The electron temperature increase at the peak of Fig. S 1 relative to the upstream temperature, ΔT_e, is up to 0.55 eV which is comparable to the experimental result of 0.8 eV. In the regions of interest motivated by the experiments, the simulations do not reproduce the measured two-component EVDFs. This suggests that 3D effects are likely to be essential to form the observed non-Maxwellian EVDFs in experiments.

To compare with Fig. 4(b) showing the lack of dependence on the gain in electron enthalpy density with guide field strength, we perform additional simulations with initial guide field strength of $B_g/B_{recx} = 10$ and 15, respectively. The density and reconnecting magnetic field profiles are qualitatively similar to the $B_g = 25$ case. We use initial electron and ion temperatures T_e and T_i given by the experimental parameters for these two discharges. For the simulation with $B_g/B_{recx} =$ 15, we use an initial T_e and T_i of 2.66 eV and 0.53 eV, respectively; for the simulation with $B_g/B_{recx} = 10$, we use an initial T_e and T_i of 3.1 eV and 0.62 eV, respectively. We use a smaller simulation domain size (compared to the $B_g/B_{recx} = 25$ case) of $L_X \times L_Y$ = 40 mm x 20 mm because (1) simulations with a larger domain produced secondary islands on both current sheets, and (2) the simulation domain does not significantly affect electron heating in the $B_g = 25$ case.

The methodology for obtaining the enthalpy density in the simulation is similar to the experiments *i.e.,* the location chosen for taking the data is about halfway between the X-point and the location where T_e peaks along the separatrix.

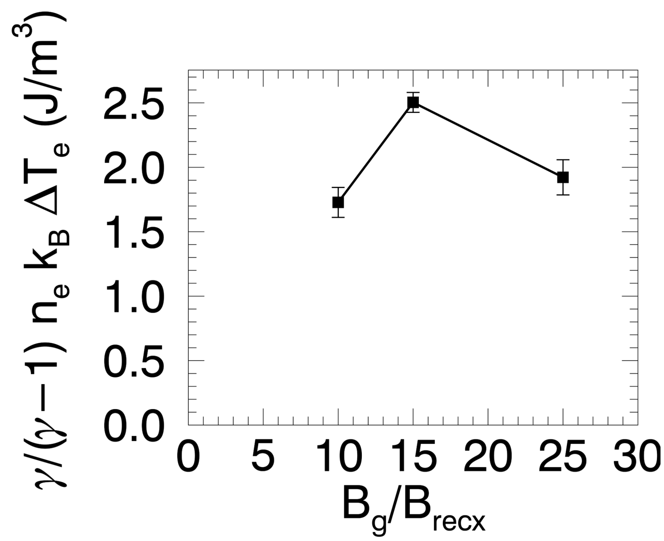

Fig. S 2. Simulation analog of Fig. 4(b), showing the electron enthalpy density gain as a function of the ratio of guide field to reconnecting field strength.

Fig. S2 shows the increase in electron enthalpy density $\gamma/(\gamma-1)n_e k_B \Delta T_e$ as a function of the ratio of guide field to reconnecting magnetic field B_g/B_{recx}. We find the simulations qualitatively agree quite well, with reasonable quantitative agreement, with the experiments as shown in Fig. 4(b) in the letter. For the scatter plots shown in Fig. S1(b) and S2, average data from the simulations is obtained over four cells and is shown as the square black boxes and the standard deviations around the average values are shown by the error bars.

Experimental temperature measurements: For our Thomson scattering system, the T_e measurement uncertainty is well below 10% of the absolute T_e value, which is essential to enable study of electron heating at sub-eV magnitudes during electron-only reconnection in PHASMA. Here, we present the experimental method used to define the uncertainty in the T_e measurements [5]. Normally, 40 shots are accumulated from repeatable discharges to obtain one EVDF. The T_e values are derived via Maxwellian fitting of EVDFs accumulated from the first N repeatable discharges, and T_e as a function of N is plotted in Fig. S3(a), red for $x = 1$ mm and black for $x = 7$ mm (corresponding to Fig. 2(a) in the main text). At the same time, the standard deviation of the

EVDF accumulated from the first N shots relative to the fitted Maxwellian EVDF involving all shots is calculated as the relative variance and is shown in Fig. S3(b). The relative variance settles down to around 0.03 for $N \geq 20$ and we use the standard deviation of T_e values for $N = 20-40$ as the uncertainty in the T_e measurements. At $x = 1$ mm, $T_e = 2.7 \pm 0.1$ eV while $T_e = 3.0 \pm 0.1$ eV at $x = 7$ mm, demonstrating that a T_e difference of 0.3 eV is statistically significant.

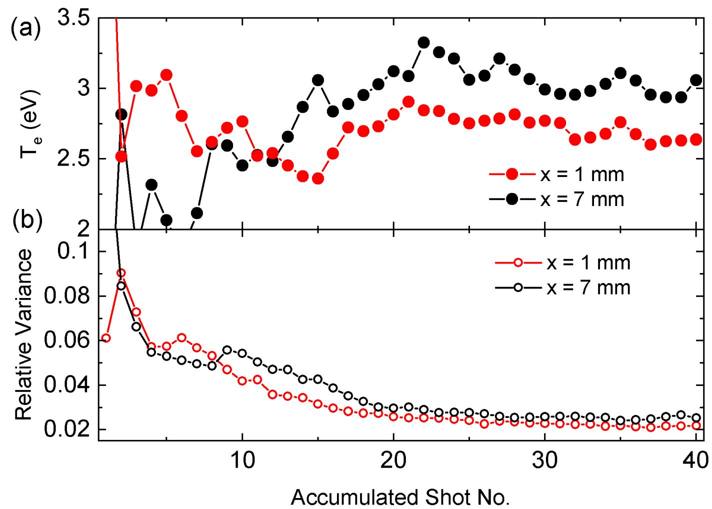

Fig. S 3. (a) The fitted T_e values and (b) relative variance for the EVDFs accumulated from the first N repeatable discharges.

We provide the measured and calculated plasma parameters for the PHASMA electron-only reconnection experiments in Table SI. To highlight the relevance of electron-only reconnection reported in this letter to satellite observations in the magnetosheath [6], we list the analogous normalized plasma parameters in Table SII.

[1] A. Zeiler, D. Biskamp, J. Drake, B. Rogers, M. Shay, and M. Scholer, Journal of Geophysical Research: Space Physics **107**, 3783 (2002).

[2] P. Sharma Pyakurel, *et al.*, Physics of Plasmas **26**, 82307 (2019).

[3] R. G. Kleva, J. F. Drake, and F. L. Waelbroeck, Physics of Plasmas **2**, 23 (1995).

[4] W. Fox, F. Sciortino, A. v. Stechow, J. Jara-Almonte, J. Yoo, H. Ji, and M. Yamada, Physical Review Letters **118**, 125002 (2017).

Reconnecting magnetic field B_{recx} (G)	15
Guide field B_g (G)	375
Plasma density n_e (m^{-3})	1×10^{19}
Electron temperature T_e (eV)	3
Ion mass M_I (u)	40 (Argon)
J_{recx} ($\mathrm{A/cm^2}$)	5
Current sheet half-thickness δ (mm)	5
Flux rope distance Δ (mm)	60
Electron inertial length $d_e = c/\sqrt{n_e e^2/m_e \varepsilon_0}$ (mm)	1.7
Ion inertial length $d_i = c/\sqrt{n_e e^2/m_i \varepsilon_0}$ (mm)	450
Electron gyro radius $\rho_e = \sqrt{k_B T_e m_e}/eB$ (mm)	0.1
Ion sound gyro radius $\rho_s = \sqrt{\gamma k_B (T_e + T_i) m_i}/eB$ (mm)	42
Ion gyro radius $\rho_i = \sqrt{k_B T_i m_i}/eB$ (mm)	12
Electron-ion collision mean free path $\lambda_{ei} = \frac{(4\pi\varepsilon_0)^2}{\pi e^4 \ln\Lambda} \cdot \frac{(k_B T_e)^2}{n_e}$ (mm)	13
Electron-neutral collision mean free path $\lambda_{en} = 1/\left(\frac{8\sqrt{\pi}}{3} n_n \sigma_{en}\right)$ (mm)	880
Electron Alfvén speed $V_{Ae} = B_{recx}/\sqrt{\mu_0 n_e m_e}$ ($\mathrm{km\,s^{-1}}$)	430
Reconnection time scale $\tau = \delta/0.1 V_{Ae}$ (μs)	0.1
Electron-ion collision time $\tau_{ei} = 1/\left(\frac{\pi e^4 \ln\Lambda}{(4\pi\varepsilon_0)^2 \sqrt{m_e}} \cdot \frac{n_e}{(k_B T_e)^{3/2}}\right)$ (μs)	0.02
Ion gyro period $\tau_{ci} = 2\pi m_i/eB$ (μs)	70
Kink growth time $\tau_{kink} = \frac{L}{B/\sqrt{\mu_0 n_e^c m_i}}$ (μs) (based on axial Alfvén time, $L = 1$ m, and central $n_e^c = 5 \times 10^{19}\ \mathrm{m^{-3}}$)	50
Spitzer electrical resistivity $\eta = 52 \frac{\ln\Lambda}{T_e[\mathrm{eV}]^{3/2}}$ (μΩ m)	100

Table. S I. Plasma parameters for electron-only reconnection on PHASMA.

	$\frac{B_g}{B_{recx}}$	$\frac{\rho_s}{d_e}$	β_e	$\frac{[\gamma/(\gamma-1)] n_e k_B \Delta T_e}{B_{recx}^2/\mu_0}$	$\frac{V_e}{V_{Ae}}$
PHASMA	10-25	30	0.01-0.05	0.7	$0.6-1$
Magnetosheath	8	23	0.3	0.5	0.45

Table. S II. Plasma parameters for PHASMA and the magnetosheath electron-only reconnection event studied by Phan et al. [6].

[5] P. Shi, P. Srivastav, C. Beatty, R. S. Nirwan, and E. E. Scime, Review of Scientific Instruments **92**, 33102 (2021).

[6] T. D. Phan, *et al.*, Nature **557**, 202 (2018).